ADVANCED MATERIALS TECHNOLOGIES
www.advmattechnol.de

Performance Improvement of Flexible Pressure Sensor Based on Ordered Hierarchical Structure Array

Shaohua Yang, Chengpeng Zhang, Jin Ji, Yongzhi Liu, Jilai Wang, and Zhenyu Shi*

Flexible pressure sensors have been extensively explored for their widespread applications in wearable electronic devices such as medical diagnosis and motion monitoring. In this paper, a facile method is adopted to prepare the ordered hierarchical structure array and then it is applied to improve the performance of capacitive flexible pressure sensors. The results indicate that the pressure sensor based on hierarchical structure array is with high sensitivity (0.382 kPa^{-1}), fast response and recovery time (26 and 25 ms), and its minimum detection pressure can reach 4 Pa. Besides, the sensor based on hierarchical structure array has also been successfully applied to the dynamic pulse monitoring of the neck, limb movement monitoring, and pressure monitoring in water cup grasping process, which shows high stability and reliability, demonstrating its broad application prospects. This research could provide useful guidance for the preparation and applications of high-performance flexible pressure sensors.

1. Introduction

The demand for flexible pressure sensors continues to expand, especially in human–computer interaction systems, electronic skins, medical care, and intelligent robots.[1–7] In order to meet these needs, high-performance flexible pressure sensors need to be developed urgently. The flexible pressure sensors can be classified into piezoelectric flexible pressure sensor,[8–10] capacitive flexible pressure sensor,[11–14] and piezoresistive flexible pressure sensor.[15–17] Compared with other types of sensors, capacitive flexible pressure sensors display the characteristics of high sensitivity, fast response time, low power consumption and stable operation, which have been widely studied.[18–20]

Various literatures have reported that flexible pressure sensors can achieve good performance by preparing the single-scale microstructures.[21–30] Shuai et al. used the pre-stretched and plasma-treated polydimethylsiloxane (PDMS) film to form a spontaneous bending structure for the preparation of microarray molds, and then the silver nanowires were coated onto the flexible substrate to construct the electrode layer of the flexible pressure sensor.[27] Zhang et al. used Ecoflex films coated with carbon nanotubes as electrodes and PDMS films with porous structures as dielectric layers, and the results showed that the micro-cone and porous structure could improve the sensitivity of the flexible pressure sensor.[28] Luo et al. developed a tilted micropillar structure array to obtain high-performance flexible pressure sensors.[29] Zhang et al. use colloidal self-assembly technology, and the surface structure of PDMS film could be changed by optimizing the size of polystyrene microspheres, thus changing the pressure sensor performance.[30]

In addition to single-scale structure array, it was found that the flexible pressure sensors with good performance could be easily gained through hierarchical structure array.[31–35] Zhu et al. used an improved seed-mediated growth method to prepare vertically aligned gold nanowires on PDMS film with micro-cone structures, and obtained flexible pressure sensors based on hierarchical structure array.[33] Mahata et al. fabricated micro-nano hierarchical structures and developed a capacitive flexible pressure sensor with excellent performance.[34] Hwang et al. prepared PDMS composites with hierarchical porous structure to further improve the sensors' performance.[35]

Herein, a facile method was adopted to prepare the ordered hierarchical structure array and then it was applied to obtain excellent capacitive flexible pressure sensors. The results showed that the hierarchical structure array could significantly improve the sensor performance, compared with the single-scale structure array. Besides, the applications of the pressure sensor based on hierarchical structure array were investigated in detail, including the dynamic pulse monitoring of the neck, limb movement monitoring, and pressure monitoring in water

S. Yang, C. Zhang, J. Ji, J. Wang, Z. Shi
Key Laboratory of High Efficiency and Clean Mechanical Manufacture of Ministry of Education, School of Mechanical Engineering
Shandong University
Jinan, Shandong 250061, China
E-mail: zhangchengpeng@sdu.edu.cn
C. Zhang, J. Wang, Z. Shi
National Demonstration Center for Experimental Mechanical Engineering Education
Shandong University
Jinan, Shandong 250061, China
C. Zhang
Suzhou Research Institute
Shandong University
Suzhou 215123, China
Y. Liu
Shandong Institute of Nonmetallic Materials
Jinan, Shandong 250031, China
The ORCID identification number(s) for the author(s) of this article can be found under https://doi.org/10.1002/admt.202200309.

DOI: 10.1002/admt.202200309

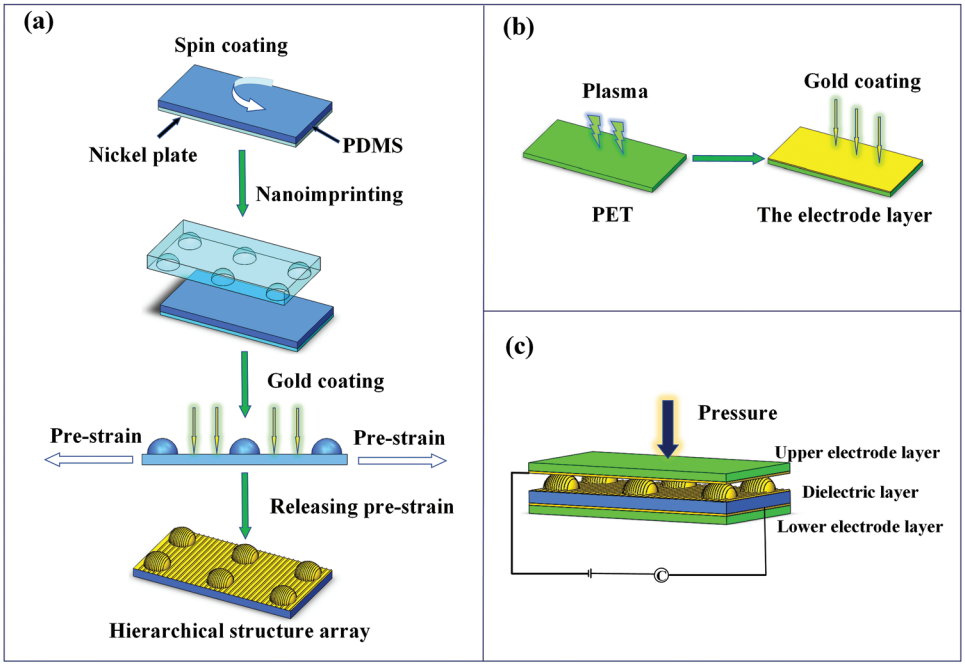

Figure 1. Fabrication process of the capacitive flexible pressure sensor: a) fabrication of PDMS dielectric layer with hierarchical structures, b) fabrication of the electrode layer, c) package of the sensors.

cup grasping process. This research could provide useful advice for the preparation and applications of flexible pressure sensors with good performance.

2. Results and Discussion

2.1. Preparation Process and Surface Topography

Figure 1 shows the preparation process of the capacitive pressure sensors based on hierarchical structures, including the fabrication of the electrode layer, preparation of PDMS dielectric layer with hierarchical structures, and package of the capacitive flexible pressure sensors.

Figure 2 displays the laser scanning microscope images of nickel mold for nanoimprinting process. As shown in Figure 2a, the nickel mold is with an ordered array of concave micro-lens structures. Moreover, the geometric parameters of the micro-lens structures are obtained through the cross-sectional analysis, which are 30 μm in length and 3.5 μm in depth, as displayed in Figure 2b.

Figure 3 presents the scanning electron microscope (SEM) images of PDMS film with microstructures. As shown in Figure 3a, the single-scale micro-lens structures prepared through nanoimprinting process are densely arranged in a regular hexagon array and exhibit excellent geometric consistency on a large view. As shown in Figure 3b, based on the single-scale micro-lens structures, the hierarchical structures array is further prepared. It can be found that a dense array of wrinkle structures is formed on the curved surfaces of the micro-lens structures.

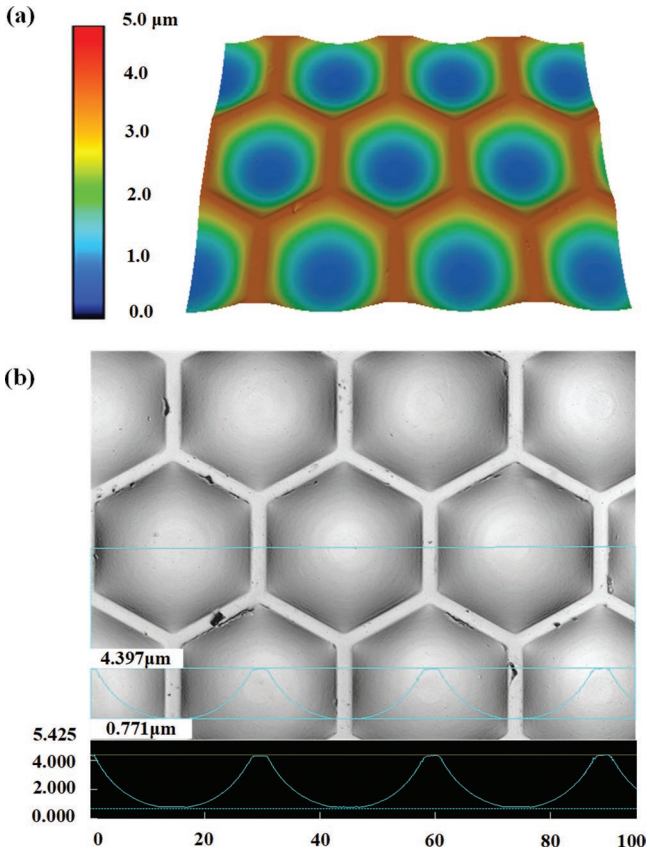

Figure 2. The images of nickel mold: a) 3D image, b) 2D image.

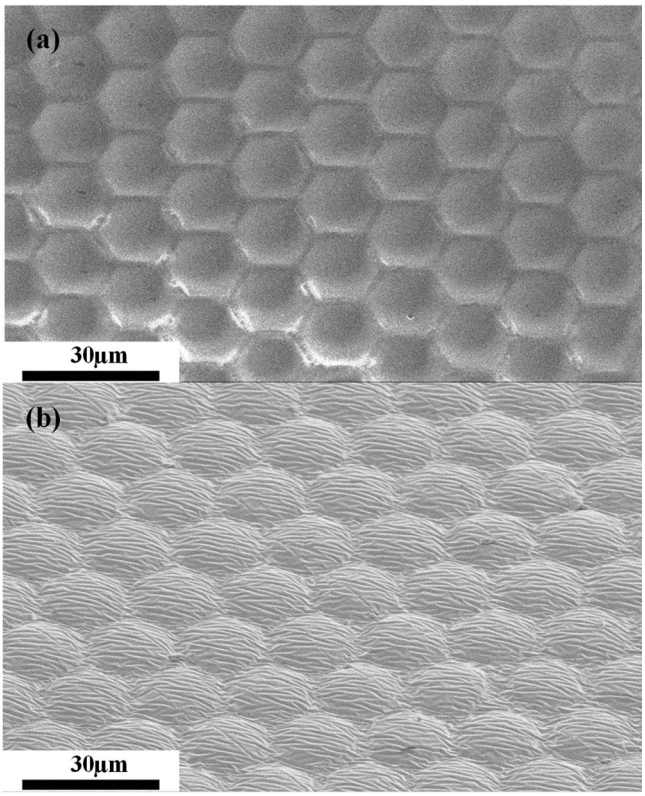

Figure 3. The SEM images of PDMS surface: a) with single-scale micro-lens structure array, b) with hierarchical structure array.

2.2. Electrical Performance

To study the effect of surface microstructures, the electrical performances of pressure sensors with single-scale micro-lens array and hierarchical structure array were investigated, as shown in **Figure 4**. The pressure of 0.25, 0.5, 1, 5, and 10 kPa was applied to the sensors with single-scale micro-lens array and hierarchical structure array for four cycles, respectively. As shown in Figure 4a, the sensor with single-scale micro-lens array has stable change in capacitance within a certain pressure range and the relative capacitance increases with the increase of pressure, which further improves the pressure response. Besides, the capacitance response curves of sensor with hierarchical structure array are displayed in Figure 4b and it can be observed that the capacitance values show greater changes than that of the sensor with single-scale micro-lens array. This can be attributed to the fact that when the pressure sensor is subjected to external pressure, the shape of the hierarchical structures deforms faster than the single-scale structures, which removes more air and causes a greater change in the dielectric constant.

Sensitivity is one of the indicators to judge whether the performance of the flexible pressure sensor is good, which can be calculated according to formulas (1) and (2),[29]

$$S = \delta(\Delta C/C_0)/\delta P \quad (1)$$

$$\Delta C = C - C_0 \quad (2)$$

Where C_0 is the primary capacitance without external force, C is the capacitance measured by device after the sensor is under pressure and P is the pressure applied to the flexible pressure sensor. As displayed in **Figure 5**a, the sensitivity of sensors with single-scale micro-lens array and hierarchical structure array in low-pressure region is 0.325 and 0.382 kPa^{-1}, respectively. It can be found that the sensitivity of the sensor with hierarchical structure array is increased by nearly 20% compared to that with single-scale micro-lens array. The reason for sensitivity difference is that when the pressure sensor is subjected to external pressure, the shape of the hierarchical structures deforms faster than the single-scale structures, which removes more air and causes a greater change in the dielectric constant, so the sensor with hierarchical structure array has higher sensitivity. Besides, it can be observed from Figure 5a that the sensitivity in low-pressure region is obviously larger than that in high-pressure region. This is because as the pressure increases, the elastic damping of the material increases, and the deformation of the PDMS dielectric layer with microstructures gradually reaches the maximum value, so the capacitance change tends to be stable and the sensitivity gradually decreases. The performance comparison of the flexible pressure sensor prepared in this paper with those reported in other literatures is also shown in **Table 1**. Moreover, the ability of the flexible pressure sensor with hierarchical structure array to detect ultra-low pressure was further measured, as displayed in Figure 5c,d. In the experiments, a sensor with a surface area of 2 cm × 2 cm was prepared, and a cephalosporin tablet with a mass of 160 mg was

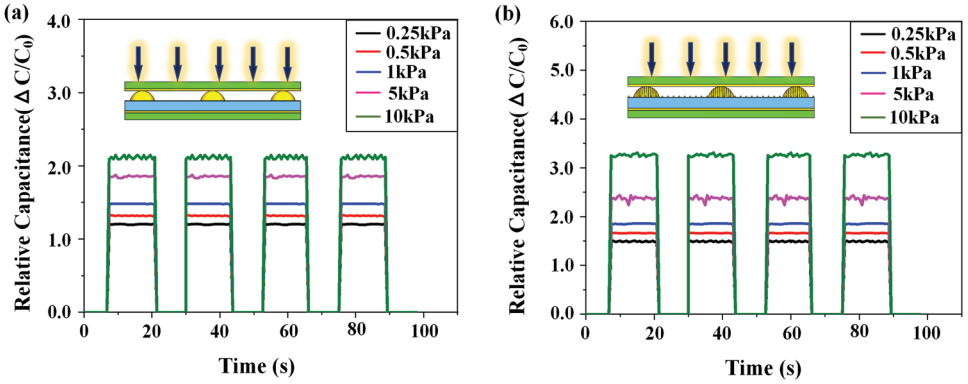

Figure 4. The capacitance response curves of pressure sensors: a) with single-scale micro-lens structure array, b) with hierarchical structure array.

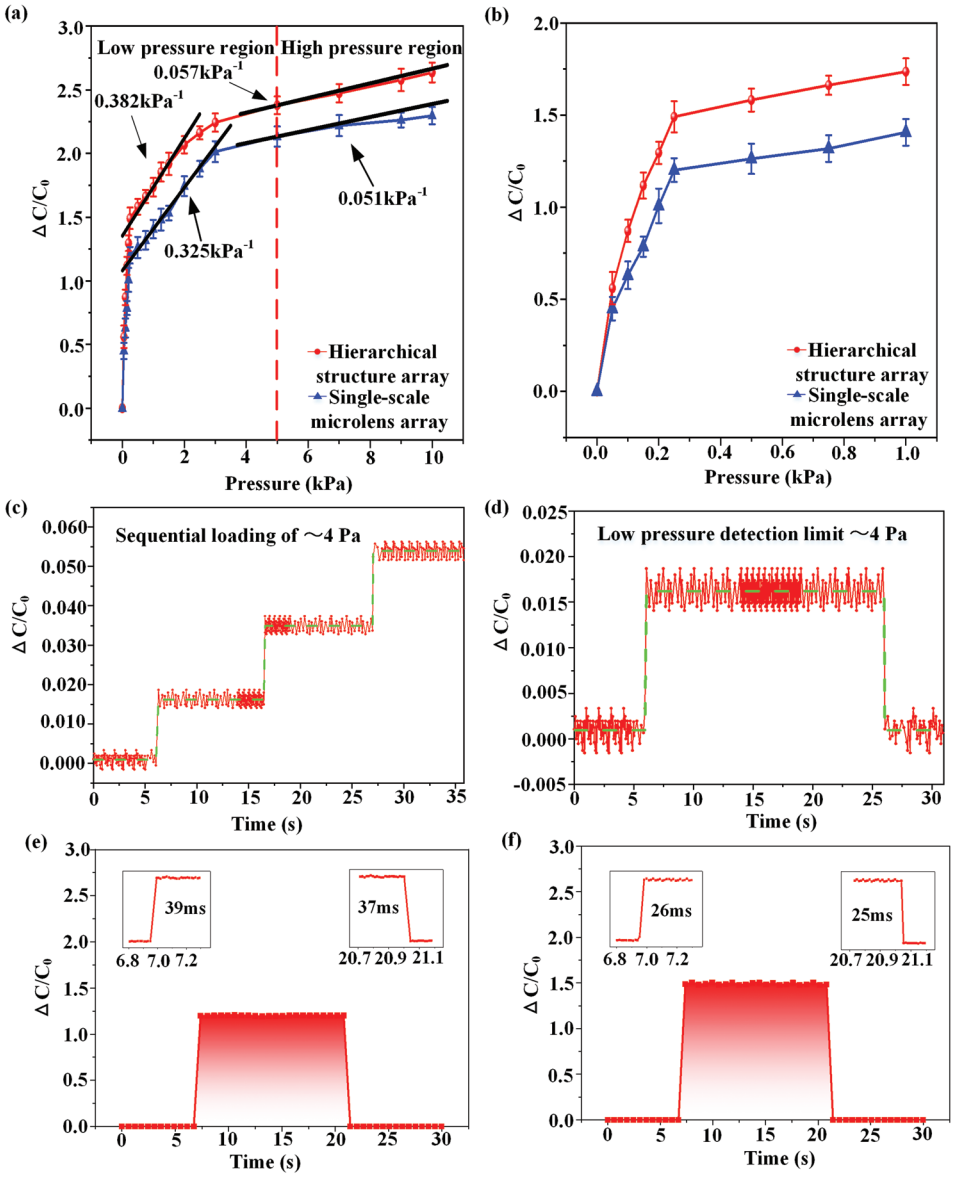

Figure 5. a) Sensitivity characterization of the pressure sensors. b) Enlarged view from (a) in the pressure range of 0–1 kPa. c,d) Low pressure detection of the sensor with hierarchical structure array. e) Response and recovery time of the sensor with single-scale micro-lens array. f) Response and recovery time of the sensor with hierarchical structure array. (e) and (f) were measured under the pressure of 0.25 kPa.

used as the detection object. It can be observed that the sensor can respond in time with the increasing number of cephalosporin tablets and the capacitance value gradually increases, indicating that the flexible pressure sensor with micro-nano hierarchical structure array can detect ultra-low pressure (4 Pa).

The response speed is another important performance of the pressure sensors. As observed from Figure 5e,f, the typical response time and recovery time of the sensor with single-scale micro-lens array are 39 and 37 ms, respectively, while the values are 26 and 25 ms for the sensor with hierarchical structure array. It can be found that the response speed of the sensor with hierarchical structure array is increased by more than 30% compared to that with single-scale micro-lens array. This phenomenon can be attributed to that the sensor based on hierarchical structure array deforms faster under the same external pressure and therefore achieves a faster response to pressure.

2.3. Applications

The pressure sensor with hierarchical structure array has high sensitivity and wide pressure range, which is applied to life signal detection and human body motion monitoring. A flexible pressure sensor was attached to the carotid artery of the neck and then the electrical signal was received through the copper wires to monitor the carotid pulse in real-time, as shown in **Figure 6**a,b. It can be seen that three peaks P_1, P_2, and P_3 can be observed, which represent the early systolic peak

Table 1. Performance comparison of various flexible pressure sensors.

Flexible pressure sensors	Sensitivity	Maximum sensing range	Reference
Sensor with a bio-mimicking hierarchical micro-nano structure	0.055 kPa^{-1}	10 kPa	[34]
Paper-based pressure sensor	0.015 kPa^{-1}	50 kPa	[36]
Sensor with Ni/Cu fabric and porous PDMS	0.023 kPa^{-1}	200 kPa	[37]
Sensor with a hierarchically porous structure	0.152 kPa^{-1}	27 kPa	[38]
Sensor of VACNT/PDMS composite conductor with irregular surface morphology	0.3 kPa^{-1}	10 kPa	[39]
Sensor with 3D voids	0.207 kPa^{-1}	20 kPa	[40]
Sensor with elastic nylon netting dielectric layer	0.33 kPa^{-1}	5 kPa	[41]
Sensor with micro-nano hierarchical structure array	0.382 kPa^{-1}	10 kPa	This work

pressure, the end-systolic peak pressure, and the diastolic pulse waveform, respectively, indicating that the sensor can be used to detect pulse. As observed in Figure 6a, the heart rate of the test subject is ≈72 beats min^{-1}, which is within the normal heart rate range, and the variation in its relative capacitance illustrates the stability and reliability of the sensor. Therefore, this sensor exhibits great potential in the application of human health detection.

In addition to carotid artery monitoring, the flexible pressure sensor is also used for limb movement monitoring. A sensor was attached to the forearm to capture the change in capacitance caused by the contraction of the forearm muscle during the grasping process. During the experiment, the sensor was attached to the forearm of the subject (23 years old, healthy), and the palm of the subject needed to be stretched from open to tight. As shown in Figure 6c, the capacitance changes sharply in the opposite direction in the process of making a fist. When the handshake process is suspended, the change of the capacitance value tends to stabilize. As the arm muscles contract tighter, the capacitance value changes more. Therefore, the sensor can be applied to sports monitoring and physical health monitoring.

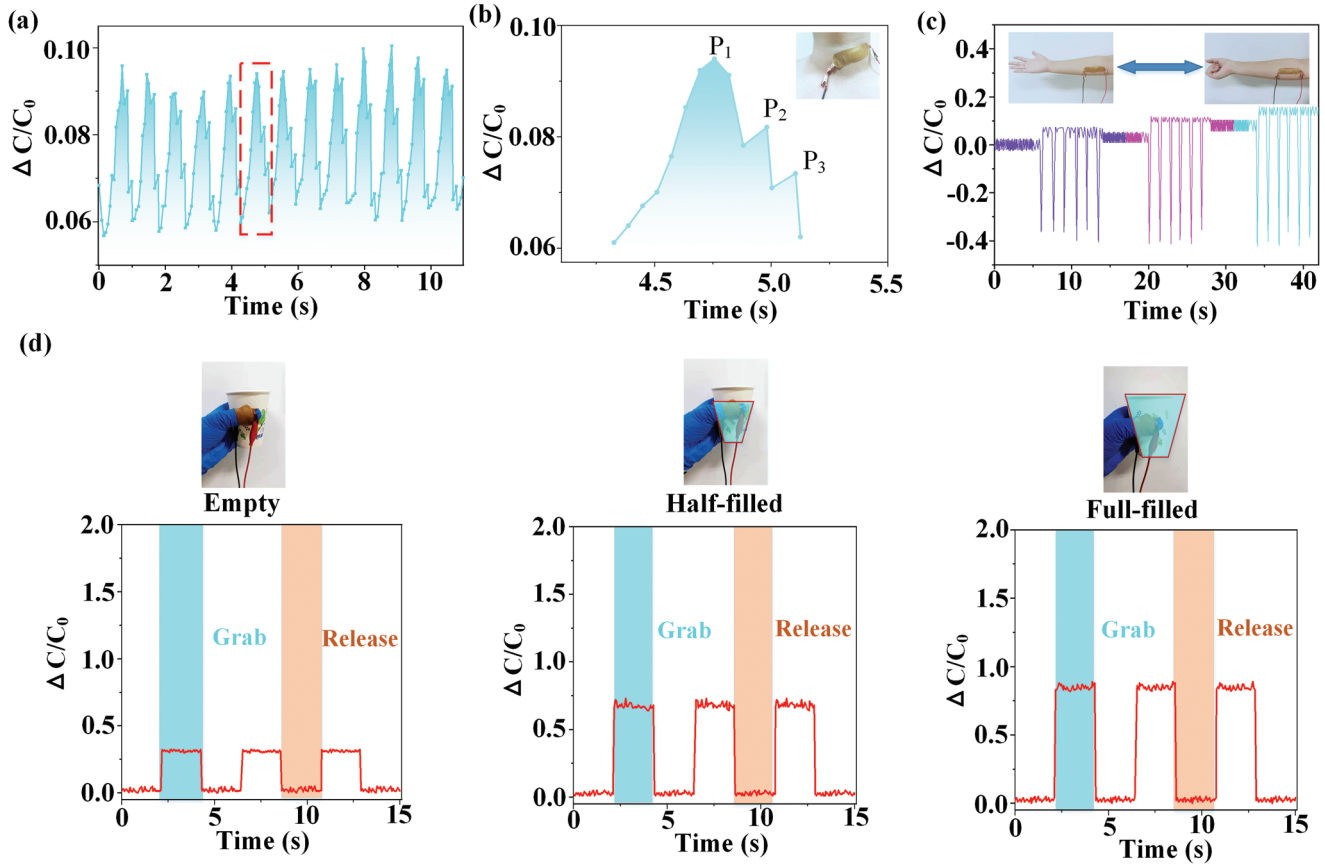

Figure 6. a) Real-time measurement of neck pulse signal with sampling frequency of 25 Hz. b) The enlarged view of one single pulse. c) Monitoring the forearm muscle contraction–expansion. d) Monitoring the water cup grasping process.

The excellent sensitivity and rapid response of the sensor with hierarchical structure array ensure that it can accurately measure the pressure between the finger and the cup wall during the grasping process. As shown in Figure 6d, the sensor was mounted on the fingertips of blue gloves, and then paper cups of different weights (3.9, 84.2, and 182.4 g) were picked and placed three times, while the capacitive signal was recorded. The results indicate that the pressure sensor in this research can be used for fingertip pressure sensing, which has important applications in the field of motion monitoring and human–computer interaction control.

3. Conclusions

In summary, a facile method was adopted to prepare the ordered hierarchical structure array and then it was applied to improve the performance of capacitive flexible pressure sensors. The results showed that the hierarchical structure array could significantly improve the performance of flexible pressure sensors compared with single-scale structure array. The pressure sensor based on hierarchical structure array was with high sensitivity (0.382 kPa^{-1}), fast response and recovery time (26 and 25 ms), and its minimum detection pressure could reach 4 Pa. Furthermore, the sensor based on hierarchical structure array was also successfully applied to the dynamic pulse monitoring of the neck, limb movement monitoring, and pressure monitoring in water cup grasping process, which showed high stability and reliability, demonstrating its huge application potential in the fields of wearable electronic devices and human health monitoring. This research could provide useful guidance for the preparation and applications of high-performance pressure sensors.

4. Experimental Section

Materials: The SYLGARD 184 PDMS used in this experiment was purchased from Dow Corning (USA), and the flexible polyethylene terephthalate (PET) film was provided by Jiangsu Kangde Xin Composite Material Co., Ltd. The nickel mold for nanoimprinting process was 2×2 cm in area.

Preparation of the PDMS Dielectric Layer: The PDMS film with microstructures was used as the dielectric layer. First, 10 g basic liquid (A liquid) and 1 g solidifying liquid (B liquid) were mixed and stirred for 5–7 min with a glass rod to obtain liquid PDMS. After stirring uniformly, the liquid PDMS was left for 5 min, and then put into a vacuum oven for 10 min. Subsequently, a spin coating device (EZ6-S, Schwan) was used to uniformly coated liquid PDMS on the smooth nickel sheet at 1500 rpm for 1 min to obtain a 0.3 mm PDMS film. With the nanoimprinting process, the microstructure array of Ni mold was transferred on the surface of the liquid PDMS. Put the PDMS and nickel mold in the oven again and vacuum treatment for 10 min, and then heat it at 120 °C for 30 min. After removing the nickel mold, the cured PDMS film with a convex micro-lens array was obtained and the height of the micro-lens array was 3.5 μm.

Based on the PDMS film with a convex micro-lens array, the hierarchical structures array was further prepared with the pre-strain method. A 15% tensile strain was applied to the PDMS film with a convex micro-lens array and then put in the magnetron sputtering apparatus (ETD-900M) to gold coating for 15 s. After releasing the pre-strain, the gold coating would buckle and deform to obtain the PDMS film with hierarchical structure array, including a convex micro-lens array and wrinkle structures, and the height of the hierarchical structure array was ≈3.8 μm.

Preparation of the Electrode Layer: The electrode layer was used to derive the electrical signals of the pressure sensors. As shown in Figure 1b, the flexible PET film was placed in the magnetron sputtering device (ETD-900M) and sprayed with gold coating for 1 min to prepare the electrode layer.

Package of the Capacitive Flexible Pressure Sensor: As seen in Figure 1c, the two electrode layers and one PDMS dielectric layer were packaged together to obtain a capacitive flexible pressure sensor.

Characterization: The surface topography of nickel mold for nanoimprinting process was measured with the laser scanning microscope (VK-X200K, KEYENCE, Japan). The surface topography of PDMS with microstructures was examined using a field emission scanning electron microscope (JSM-7610F, JEOL, Japan) at an accelerating voltage of 5 KV. The capacitance measurements were performed with a digit multimeter (DMM6500, Keithley, USA).

Acknowledgements

This work was supported by the Shandong Provincial Natural Science Foundation (ZR2021QE129), the Natural Science Foundation of Jiangsu Province (BK20190202), the Research Project of State Key Laboratory of Mechanical System and Vibration (MSV202102), and the China Postdoctoral Science Foundation (2021M691926).

Conflict of Interest

The authors declare no conflict of interest.

Data Availability Statement

The data that support the findings of this study are available from the corresponding author upon reasonable request.

Keywords

capacitive pressure sensor, flexible sensor, hierarchical structures

Received: February 27, 2022
Revised: May 27, 2022
Published online:

[1] G. Y. Bae, J. T. Han, G. Lee, S. Lee, S. W. Kim, S. Park, J. Kwon, S. Jung, K. Cho, *Adv. Mater.* **2018**, *30*, 1803388.
[2] C. M. Boutry, A. Nguyen, Q. O. Lawal, A. Chortos, S. Rondeau Gagne, Z. Bao, *Adv. Mater.* **2015**, *27*, 6954.
[3] L. Cheng, R. Wang, X. Hao, G. Liu, *Sensors* **2021**, *21*, 289.
[4] J, Ji , C. Zhang, S. Yang, Y. Liu, J. Wang, Z. Shi, *ACS Appl. Mater. Interfaces* **2022**, *14*, 24059.
[5] Y. Pang, K. Zhang, Z. Yang, S. Jiang, Z. Ju, Y. Li, X. Wang, D. Wang, M. Jian, Y. Zhang, R. Liang, H. Tian, Y. Yang, T. L. Ren, *ACS Nano* **2018**, *12*, 2346.
[6] D. Y. Park, D. J. Joe, D. H. Kim, H. Park, J. H. Han, C. K. Jeong, H. Park, J. G. Park, B. Joung, K. J. Lee, *Adv. Mater.* **2017**, *29*, 1702308.
[7] H. Luo, G. Pang, K. Xu, Z. Ye, H. Yang, G. Yang, *Adv. Mater. Technol.* **2021**, *6*, 2100616.

[8] X. Hou, S. Zhang, J. Yu, M. Cui, J. He, L. Li, X. Wang, X. Chou, *Energy Technol.* **2020**, *8*, 1901242.
[9] Y. Qiu, S. Sun, C. Xu, Y. Wang, Y. Tian, A. Liu, X. Hou, H. Chai, Z. Zhang, H. Wu, *J. Mater. Chem. C* **2021**, *9*, 584.
[10] Y. Yang, H. Pan, G. Xie, Y. Jiang, C. Chen, Y. Su, Y. Wang, H. Tai, *Sens. Actuators, A* **2020**, *301*, 111789.
[11] Z. Luo, J. Chen, Z. Zhu, L. Li, Y. Su, W. Tang, O. M. Omisore, L. Wang, H. Li, *ACS Appl. Mater. Interfaces* **2021**, *13*, 7635.
[12] M. Pruvost, W. J. Smit, C. Monteux, P. Poulin, A. Colin, *npj Flexible Electron.*. **2019**, *3*, 7.
[13] H. Zhou, M. Wang, X. Jin, H. Liu, J. Lai, H. Du, W. Chen, A. Ma, *ACS Appl. Mater. Interfaces* **2021**, *13*, 1441.
[14] W. Asghar, F. Li, Y. Zhou, Y. Wu, Z. Yu, S. Li, D. Tang, X. Han, J. Shang, Y. Liu, R. W. Li, *Adv. Mater. Technol.* **2020**, *5*, 1441.
[15] D. Kannichankandy, P. M. Pataniya, S. Narayan, V. Patel, C. K. Sumesh, K. D. Patel, G. K. Solanki, V. M. Pathak, *Synth. Met.* **2021**, *273*, 116697.
[16] X. Pang, Q. Zhang, Y. Shao, M. Liu, D. Zhang, Y. Zhao, *Sensors* **2021**, *21*, 1130.
[17] G. Yang, M. Z. Tian, P. Huang, Y. F. Fu, Y. Q. Li, Y. Q. Fu, X. Q. Wang, Y. Li, N. Hu, S. Y. Fu, *Carbon* **2021**, *173*, 736.
[18] S. Chen, B. Zhuo, X. Guo, *ACS Appl. Mater. Interfaces* **2016**, *8*, 20364.
[19] S. Kang, J. Lee, S. Lee, S. Kim, J. K. Kim, H. Algadi, S. Al-Sayari, D.-E. Kim, D. Kim, T. Lee, *Adv. Electron. Mater.* **2016**, *2*, 1600356.
[20] S. Sharma, A. Chhetry, S. Zhang, H. Yoon, C. Park, H. Kim, M. Sharifuzzaman, X. Hui, J. Y. Park, *ACS Nano* **2021**, *15*, 4380.
[21] R. Li, Q. Zhou, Y. Bi, S. Cao, X. Xia, A. Yang, S. Li, X. Xiao, *Sens. Actuators, A* **2021**, *321*, 112425.
[22] C. Zhang, S. Chen, J. Wang, Z. Shi, L. Du, *Adv. Mater. Interfaces* **2022**, *9*, 2102468.
[23] S. C. Mannsfeld, B. C. Tee, R. M. Stoltenberg, C. V. Chen, S. Barman, B. V. Muir, A. N. Sokolov, C. Reese, Z. Bao, *Nat. Mater.* **2010**, *9*, 859.
[24] J. Yang, S. Luo, X. Zhou, J. Li, J. Fu, W. Yang, D. Wei, *ACS Appl. Mater. Interfaces* **2019**, *11*, 14997.
[25] C. Zhang, S. Chen, Z. Jiang, Z. Shi, J. Wang, L. Du, *ACS Appl. Mater. Interfaces* **2021**, *13*, 29222.
[26] X. Zhang, Y. Hu, H. Gu, P. Zhu, W. Jiang, G. Zhang, R. Sun, C. P. Wong, *Adv. Mater. Technol.* **2019**, *4*, 1900367.
[27] X. Shuai, P. Zhu, W. Zeng, Y. Hu, X. Liang, Y. Zhang, R. Sun, C. P. Wong, *ACS Appl. Mater. Interfaces* **2017**, *9*, 26314.
[28] Z. Zhang, X. Gui, Q. Hu, L. Yang, R. Yang, B. Huang, B. R. Yang, Z. Tang, *Adv. Electron. Mater.* **2021**, *7*, 2100174.
[29] Y. Luo, J. Shao, S. Chen, X. Chen, H. Tian, X. Li, L. Wang, D. Wang, B. Lu, *ACS Appl. Mater. Interfaces* **2019**, *11*, 17796.
[30] Y. Zhang, Y. Hu, P. Zhu, F. Han, Y. Zhu, R. Sun, C. P. Wong, *ACS Appl. Mate. Interfaces* **2017**, *9*, 35968.
[31] O. Atalay, A. Atalay, J. Gafford, C. Walsh, *Adv. Mater. Technol.* **2017**, *3*, 1700237.
[32] W. Li, X. Jin, X. Han, Y. Li, W. Wang, T. Lin, Z. Zhu, *ACS Appl. Mater. Interfaces* **2021**, *13*, 19211.
[33] B. Zhu, Y. Ling, L. W. Yap, M. Yang, F. Lin, S. Gong, Y. Wang, T. An, Y. Zhao, W. Cheng, *ACS Appl. Mater. Interfaces* **2019**, *11*, 29014.
[34] C. Mahata, H. Algadi, J. Lee, S. Kim, T. Lee, *Measurement* **2020**, *151*, 107095.
[35] J. Hwang, Y. Kim, H. Yang, J. H. Oh, *Composites, Part B* **2021**, *211*, 108607.
[36] W. Li, L. Xiong, Y. Pu, Y. Quan, S. Li, *Nanoscale Res. Lett.* **2019**, *14*, 183.
[37] S. Li, K. Dong, R. Li, X. Huang, T. Chen, X. Xiao, *Sens. Actuators, A* **2020**, *312*, 112106.
[38] G. Ge, Y. Cai, Q. Dong, Y. Zhang, J. Shao, W. Huang, X. Dong, *Nanoscale* **2018**, *10*, 10033.
[39] K. H. Kim, S. K. Hong, N. S. Jang, S. H. Ha, H. W. Lee, J. M. Kim, *ACS Appl. Mater. Interfaces* **2017**, *9*, 17499.
[40] L. Huang, Z. Yu, J. Chen, D. Tang, *ACS Appl. Bio Mater.* **2020**, *3*, 9156.
[41] Z. He, W. Chen, B. Liang, C. Liu, L. Yang, D. Lu, Z. Mo, H. Zhu, Z. Tang, X. Gui, *ACS Appl. Mater. Interfaces* **2018**, *10*, 12816.